materials

Supplementary Materials

Synthesis, polymorphism and thermal decomposition process of $(n\text{-}C_4H_9)_4NRE(BH_4)_4$ for *RE* = Ho, Tm and Yb

Wojciech Wegner [1,2,*] and Tomasz Jaroń [2,*]

[1] College of Inter-Faculty Individual Studies in Mathematics and Natural Sciences, University of Warsaw, Banacha 2c, 02-097 Warsaw, Poland
[2] Centre of New Technologies, University of Warsaw, Banacha 2c, 02-097 Warsaw, Poland
* Correspondence: w.wegner@cent.uw.edu.pl (W.W.), t.jaron@cent.uw.edu.pl. (T.J.)

Contents

Citation: Wegner, W.; Jaroń, T.; Synthesis, Polymorphism and Thermal Decomposition Process of $(n\text{-}C_4H_9)_4NRE(BH_4)_4$ for *RE* = Ho, Tm and Yb. *Materials* **2021**, *14*, 1329. https://doi.org/10.3390/ma14061329

Academic Editor: Jacques Huot

Received: 27 January 2021
Accepted: 4 March 2021
Published: 10 March 2021

Publisher's Note: MDPI stays neutral with regard to jurisdictional claims in published maps and institutional affiliations.

Copyright: © 2021 by the authors. Submitted for possible open access publication under the terms and conditions of the Creative Commons Attribution (CC BY) license (http://creativecommons.org/licenses/by/4.0/).

1. PXRD Patterns, Rietveld Refinement and Structural Information

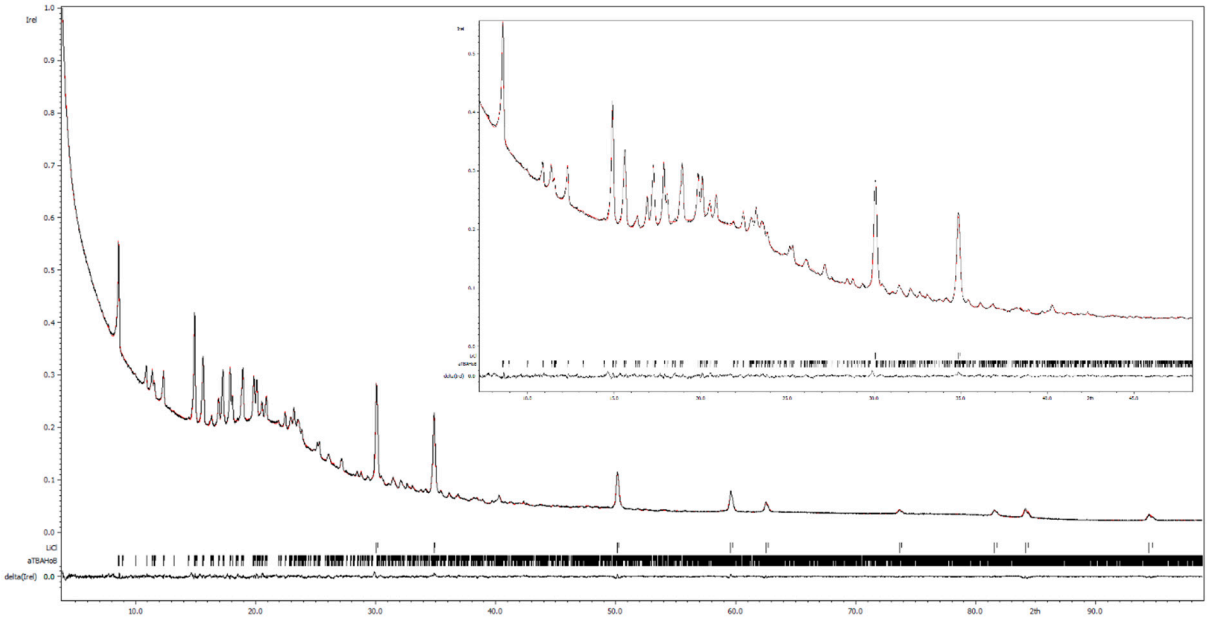

Figure S1. Rietveld refinement for as-milled sample **Ho**. Black curve represents experimental data, red curve – calculated profile. The position of the Bragg reflections has been marked and the difference curve (between the experimental and calculated profiles) are plotted at the bottom. Inset: the low angle region. GOF = 1.73; Rp = 0.73; wRp = 1.06. Wavelength: Cu ($K_{\alpha 1}$ and $K_{\alpha 2}$). Bragg reflections marked, from top to bottom, for: LiCl and α-TBAHoB.

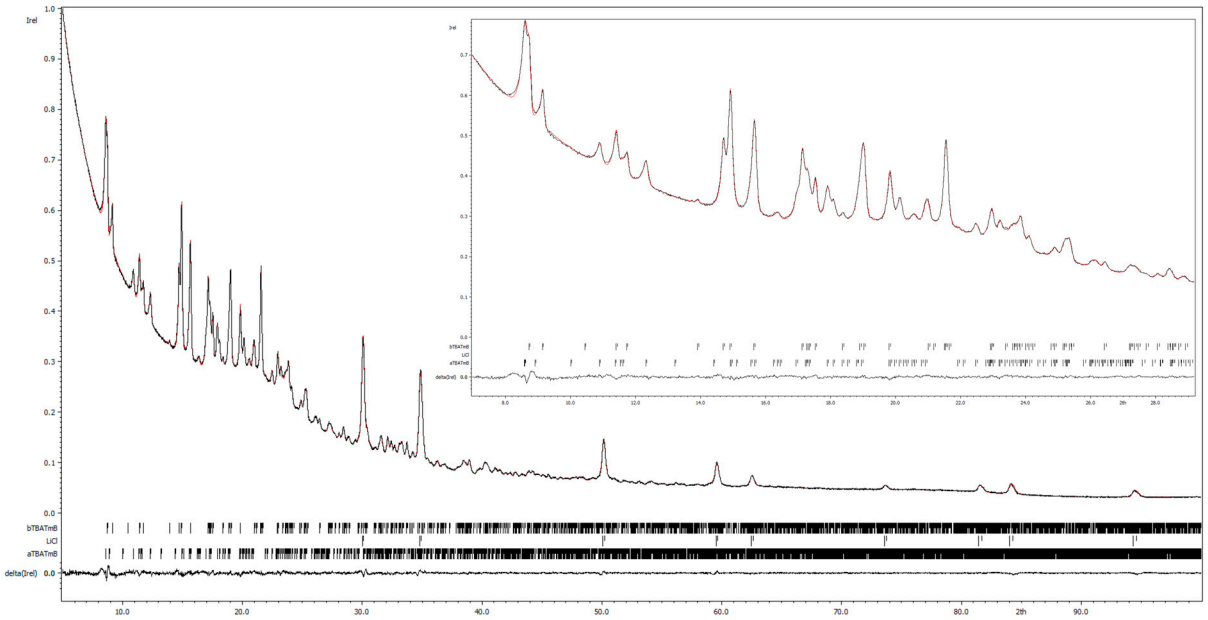

Figure S2. Rietveld refinement for as-milled sample **Tm**. Black curve represents experimental data, red curve – calculated profile. The position of the Bragg reflections has been marked and the difference curve (between the experimental and calculated profiles) are plotted at the bottom. Inset: the low angle region. GOF = 1.64; Rp = 0.69; wRp = 0.97. Wavelength: Cu ($K_{\alpha 1}$ and $K_{\alpha 2}$). Bragg reflections marked, from top to bottom, for: β-TBATmB, LiCl and α-TBATmB.

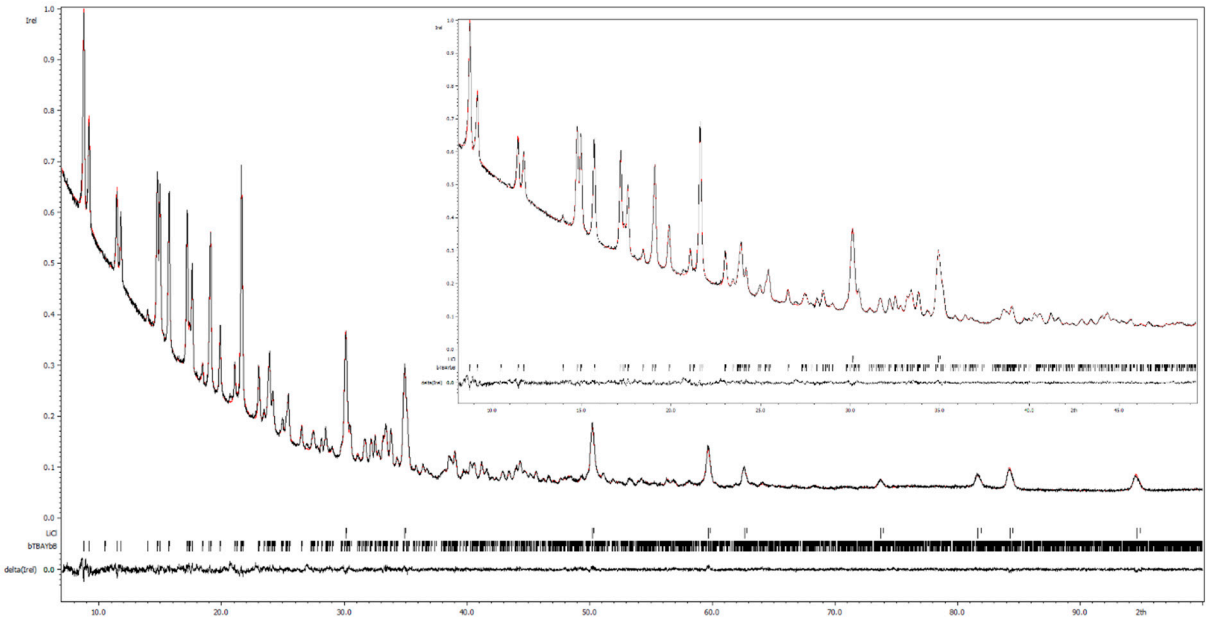

Figure S3. Rietveld refinement for as-milled sample **Yb**. Black curve represents experimental data, red curve – calculated profile. The position of the Bragg reflections has been marked and the difference curve (between the experimental and calculated profiles) are plotted at the bottom. Inset: the low angle region. GOF = 0.03; Rp = 1.29; wRp = 1.71. Wavelength: Cu ($K_{\alpha 1}$ and $K_{\alpha 2}$). Bragg reflections marked, from top to bottom, for: LiCl and β-TBAYbB.

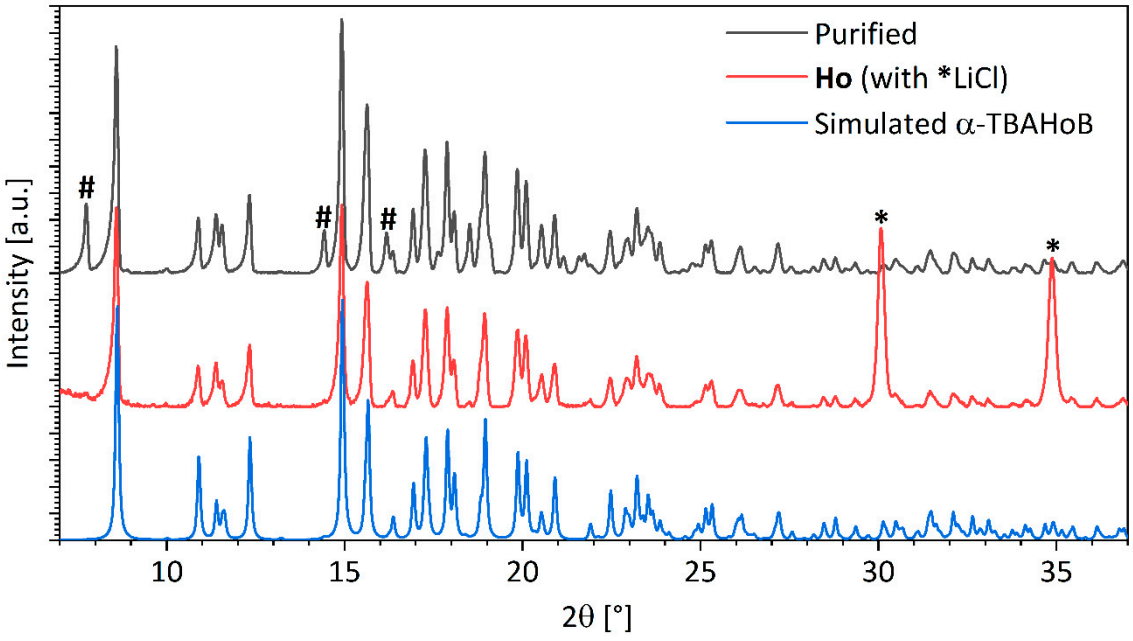

Figure S4. PXRD patterns with subtracted backgrounds for as-milled **Ho** sample (containing LiCl, marked *), purified **Ho** (with unknown impurities, marked #) and simulated pattern of α-TBAHoB (from cif, crystal structure obtained from Rietvield refinement).

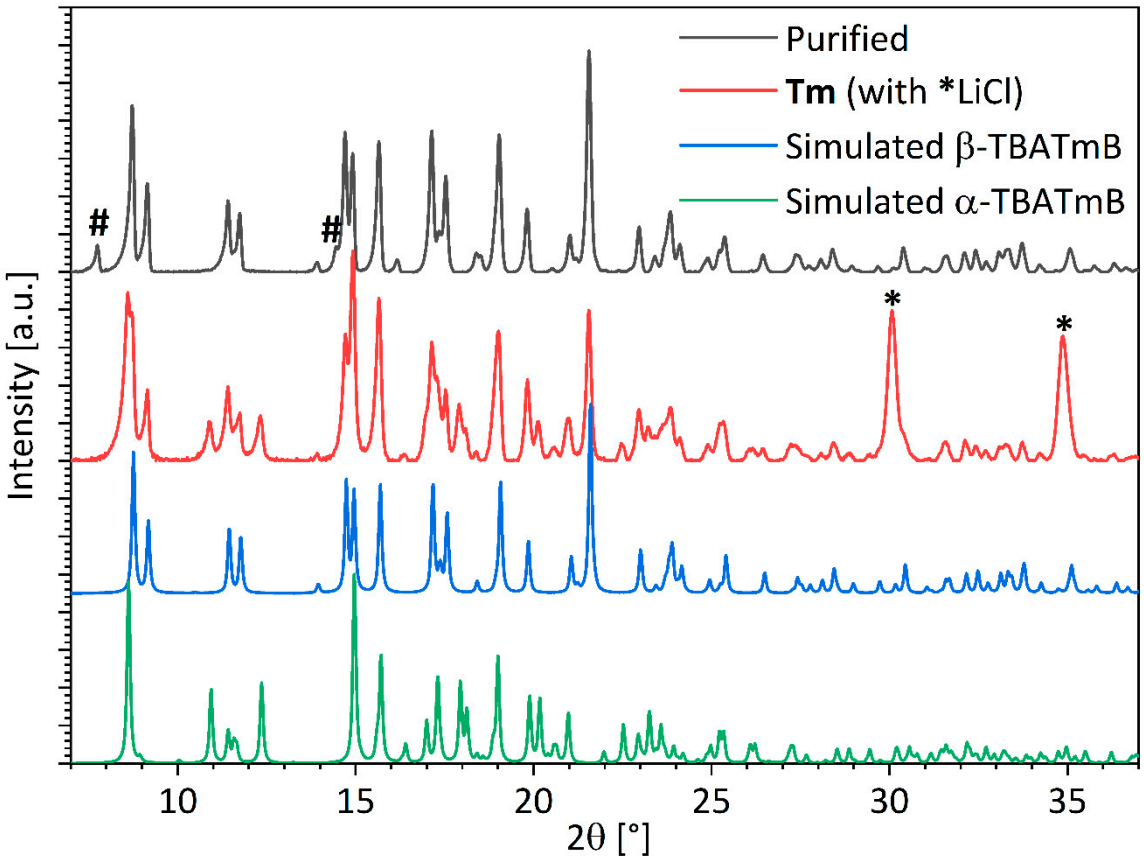

Figure S5. PXRD patterns with subtracted backgrounds for as-milled **Tm** sample (containing LiCl, marked *), purified **Tm** (with unknown impurities, marked #) and simulated patterns of α-TBATmB and β-TBATmB (from cifs, crystal structures obtained from Rietvield refinement).

Table S1. supplementary to **Table 2**. Unit cell dimensions for TBA*RE*B, *RE* = Y, Ho, Tm, Yb, Sc. 100/200/300 K obtained from SC-XRD, RT from PXRD.

Compd.	**α-TBAYB [41]**		**α-TBAHoB**		**α-TBATmB**	**β-TBAHoB**			**β-TBATmB**				**β-TBAYbB**		**β-TBAScB [42]**
RE^{3+} r[1] [Å]	0.900		0.901		0.880	0.901			0.880				0.868		0.745
spc. group	*P*2$_1$/c		*P*2$_1$/c		*P*2$_1$/c	*P*nna			*P*nna				*P*nna		*P*nna
T [K]	100	RT	100	RT	RT	100	200	300	100	200	300	RT	100	RT	RT
a [Å]	11.0453(5)	11.4181(10)	11.039(3)	11.4218(9)	11.4063(18)	18.5597(8)	18.9387(15)	19.3238(12)	18.5303(5)	18.9730(6)	19.3409(16)	19.287(3)	18.5673(9)	19.2235(10)	19.1399(10)
b [Å]	20.0099(9)	20.510(3)	19.999(2)	20.553(2)	20.545(4)	11.9188(3)	11.9783(8)	12.0529(5)	11.8902(4)	11.9295(4)	12.0279(11)	12.0317(17)	11.8735(5)	11.9943(6)	11.8849(6)
c [Å]	14.7204(8)	15.2811(19)	14.708(4)	15.3049(17)	15.319(3)	11.7871(4)	11.8153(9)	11.8820(6)	11.7514(3)	11.7754(4)	11.8749(12)	11.8591(19)	11.7096(5)	11.8244(6)	11.7325(6)
β [°]	127.980(5)	129.464(8)	128.02(4)	129.433(7)	129.423(12)	90	90	90	90	90	90	90	90	90	90
V [Å^3]	2564.44	2762.77	2558.1(10)	2775.0(5)	2773.1(10)	2607.42(16)	2680.3(3)	2767.4(3)	2589.17(13)	2665.23(15)	2762.5(4)	2751.9(7)	2581.5(2)	2726.4(2)	2668.9(2)
Z	4		4		4	4			4				4		4

[1] Effective ionic radius (6-coordinate, octahedral environment) from [54]

Compd.	**α-TBAYB [41]**		**α-TBAHoB**		**α-TBATmB**
RE^{3+} r[1] [Å]	0.900		0.901		0.880
spc. group	*P*2$_1$/c		*P*2$_1$/c		*P*2$_1$/c
T [K]	100	RT	100	RT	RT
a [Å]	11.0453(5)	11.4181(10)	11.039(3)	11.4218(9)	11.4063(18)
b [Å]	20.0099(9)	20.510(3)	19.999(2)	20.553(2)	20.545(4)
c [Å]	14.7204(8)	15.2811(19)	14.708(4)	15.3049(17)	15.319(3)
β [°]	127.980(5)	129.464(8)	128.02(4)	129.433(7)	129.423(12)
V [Å^3]	2564.44	2762.77	2558.1(10)	2775.0(5)	2773.1(10)
Z	4		4		4

Compd.	**β-TBAHoB**			**β-TBATmB**				**β-TBAYbB**		**β-TBAScB [42]**
RE^{3+} r[1] [Å]	0.901			0.880				0.868		0.745
spc. group	*P*nna			*P*nna				*P*nna		*P*nna
T [K]	100	200	300	100	200	300	RT	100	RT	RT
a [Å]	18.5597(8)	18.9387(15)	19.3238(12)	18.5303(5)	18.9730(6)	19.3409(16)	19.287(3)	18.5673(9)	19.2235(10)	19.1399(10)
b [Å]	11.9188(3)	11.9783(8)	12.0529(5)	11.8902(4)	11.9295(4)	12.0279(11)	12.0317(17)	11.8735(5)	11.9943(6)	11.8849(6)
c [Å]	11.7871(4)	11.8153(9)	11.8820(6)	11.7514(3)	11.7754(4)	11.8749(12)	11.8591(19)	11.7096(5)	11.8244(6)	11.7325(6)
β [°]	90	90	90	90	90	90	90	90	90	90
V [Å^3]	2607.42(16)	2680.3(3)	2767.4(3)	2589.17(13)	2665.23(15)	2762.5(4)	2751.9(7)	2581.5(2)	2726.4(2)	2668.9(2)
Z	4			4				4		4

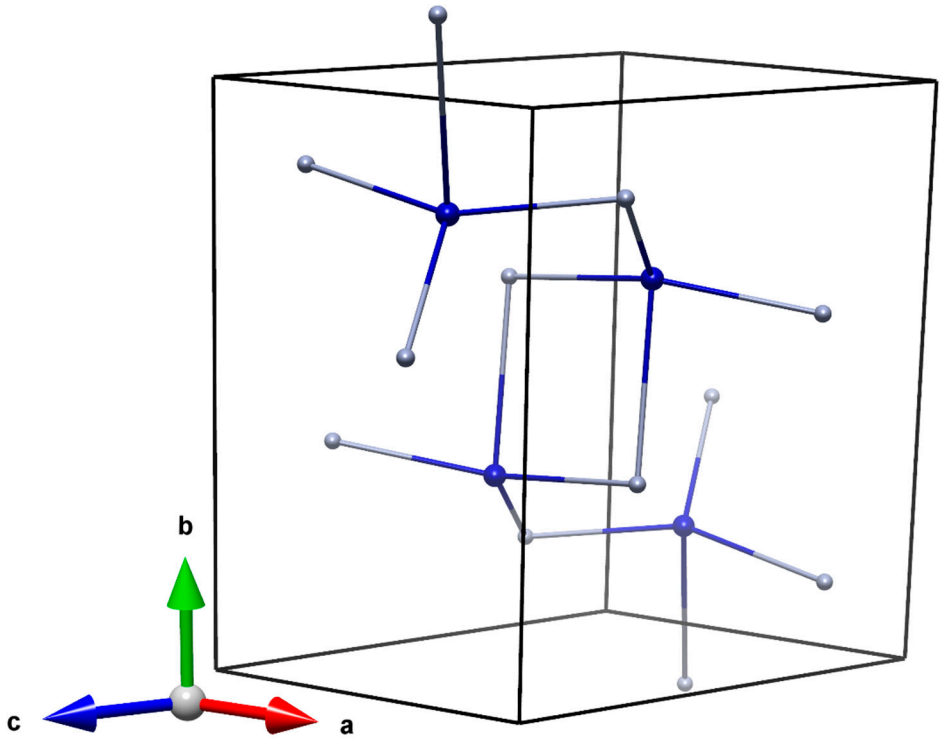

Figure S6. Nitrogen centers of TBA^+ cations (marked gray) and RE^{3+} (here *RE* = Tm, marked blue) in α-TBA*RE*B.

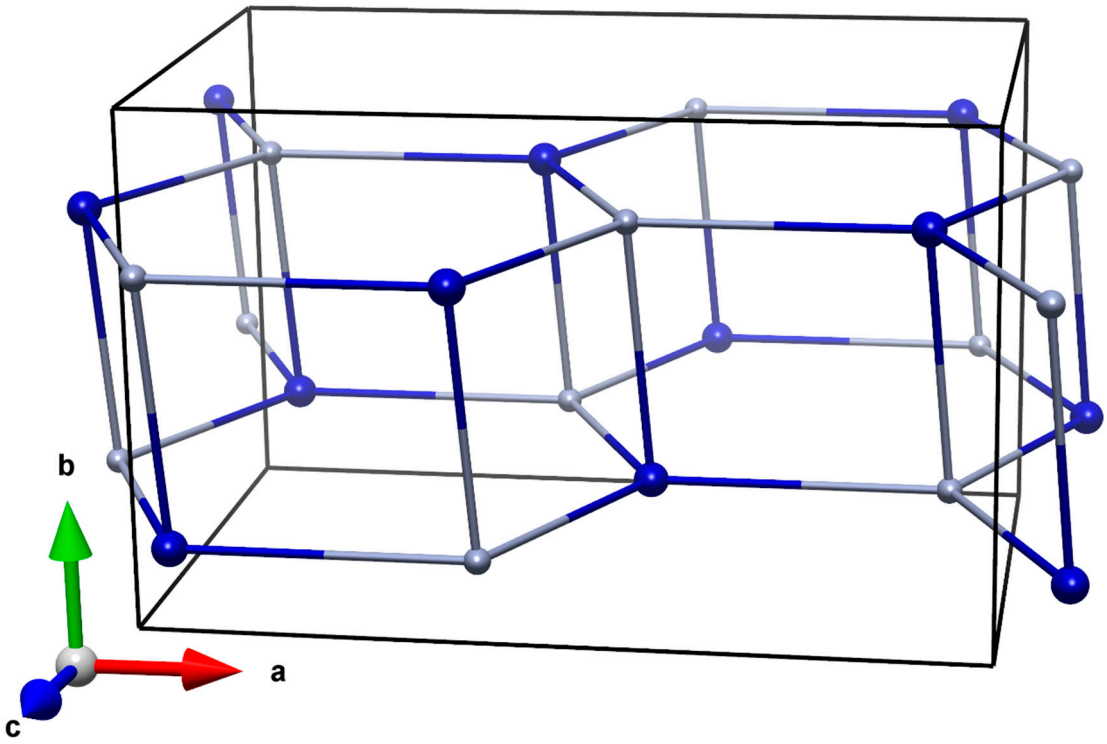

Figure S7. Honeycomb-like structure of nitrogen centers of TBA^+ cations (marked gray) and RE^{3+} (here *RE* = Tm, marked blue) in β-TBA*RE*B.

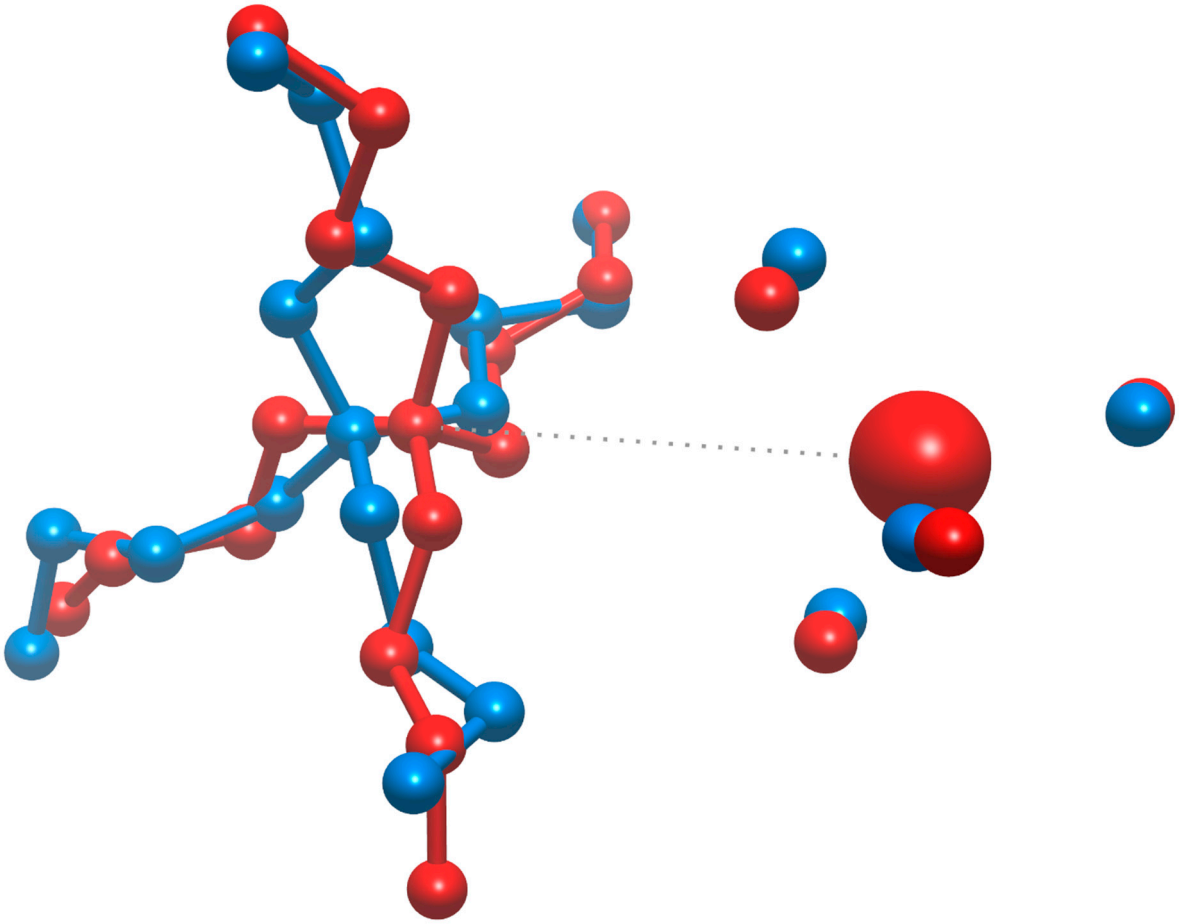

Figure S8. *RE*…N distances for α-TBAHoB (atoms marked red) and α-TBATmB (atoms marked blue), crystal structures obtained from PXRD. Left: TBA^+, right: $[RE(BH_4)_4]^-$. H atoms are not included.

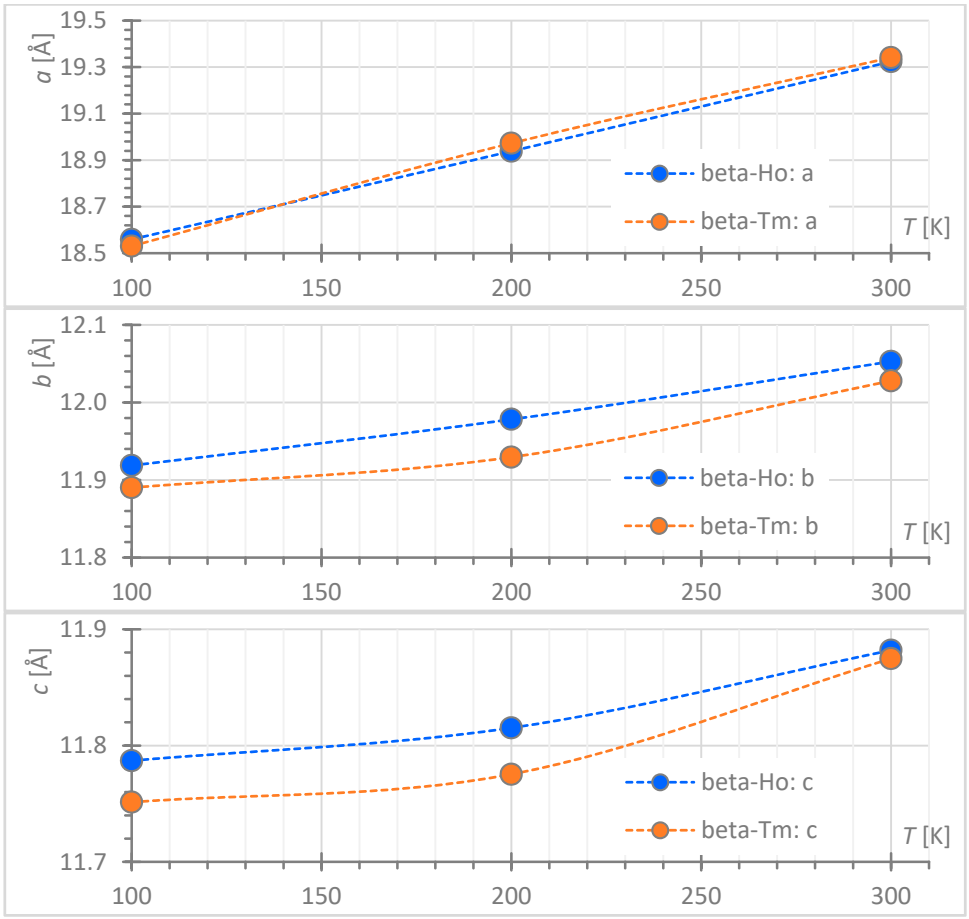

Figure S9. Evolution of *a*, *b*, and *c* lattice parameters of β-TBAHoB and β-TBATmB in the function of temperature. SC-XRD data.

2. Thermal decomposition

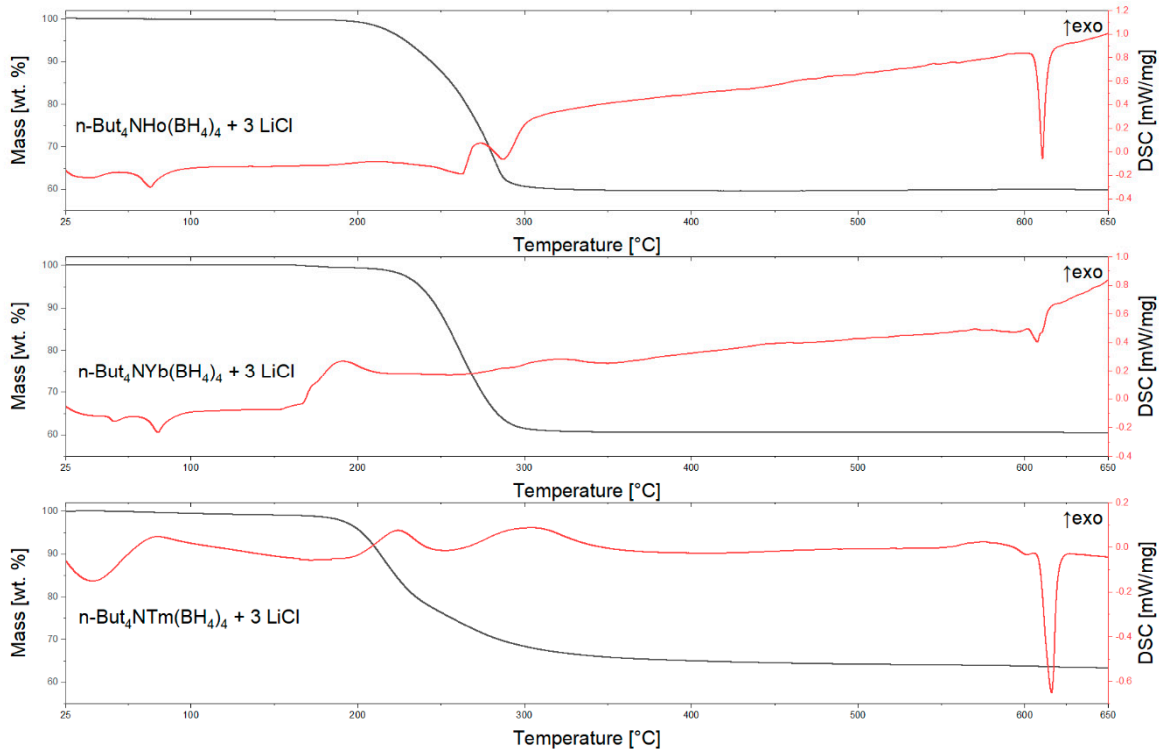

Figure S10. TGA/DSC curves of the as-milled samples (a) **Ho**, (b) **Yb** and (c) **Tm**, up to 650 °C.

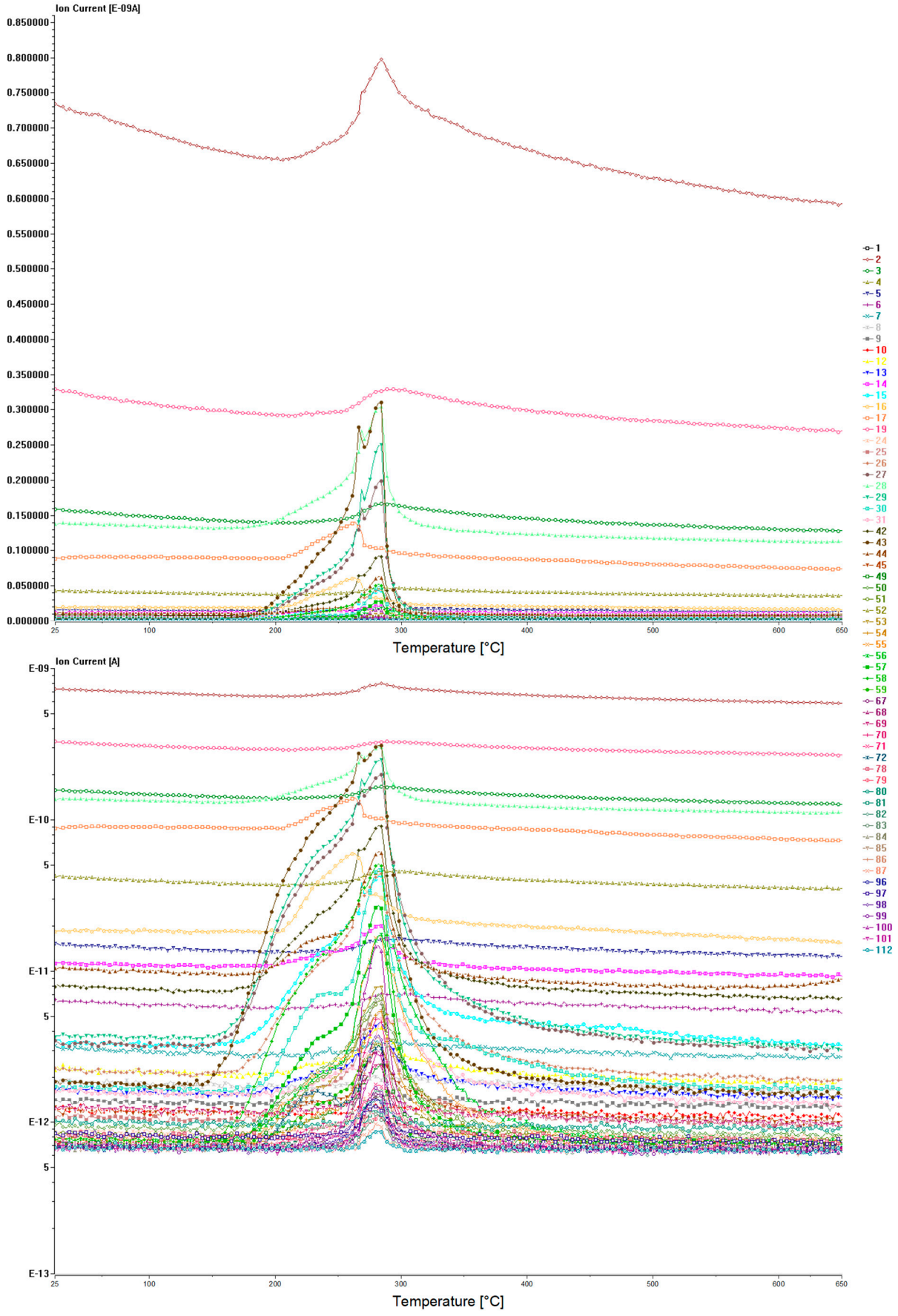

Figure S11. MS spectrum for **Ho** sample. Top: linear scale; bottom: logarithmic scale; right: m/z value legend.

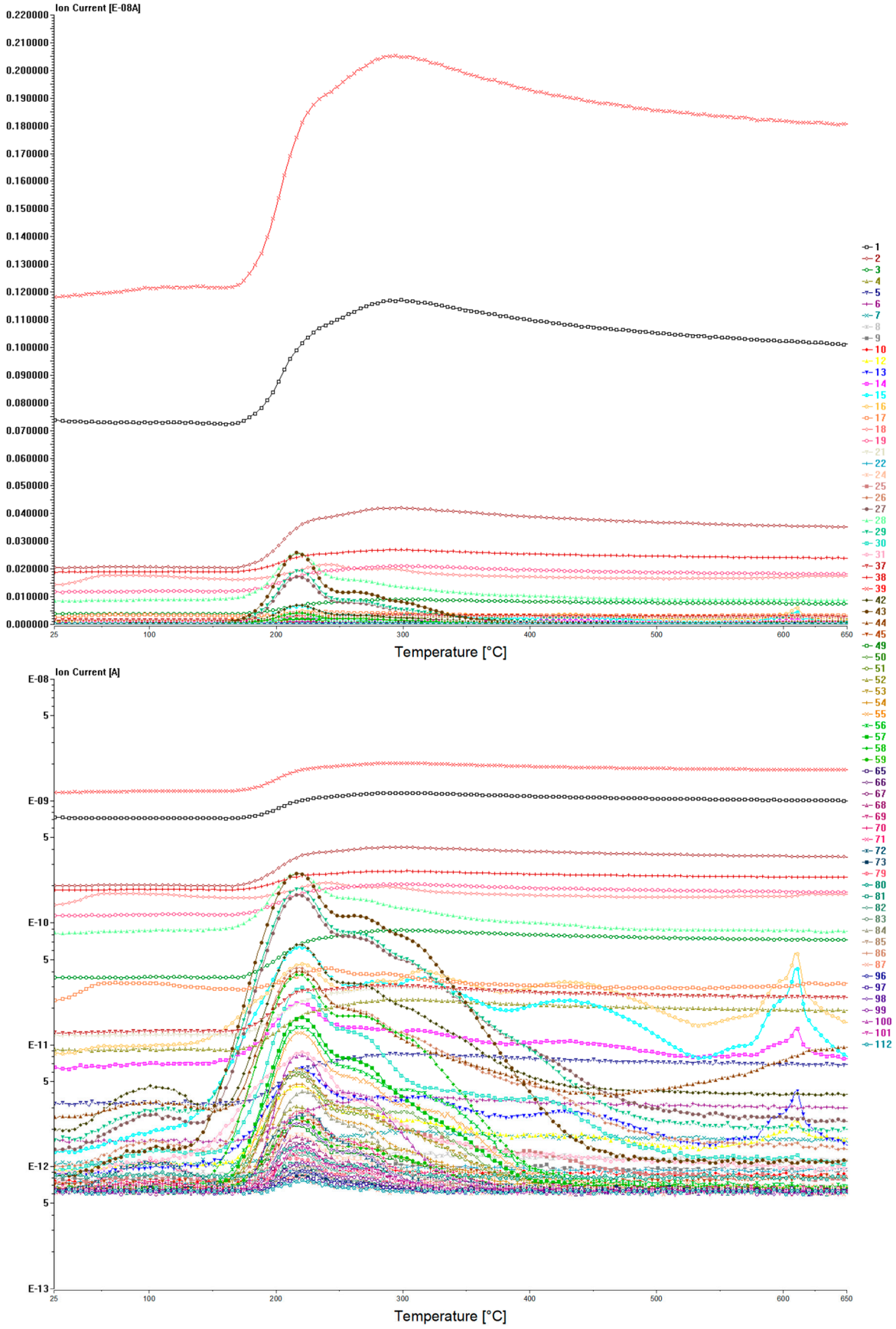

Figure S12. MS spectrum for **Tm** sample. Top: linear scale; bottom: logarithmic scale; right: m/z value legend.

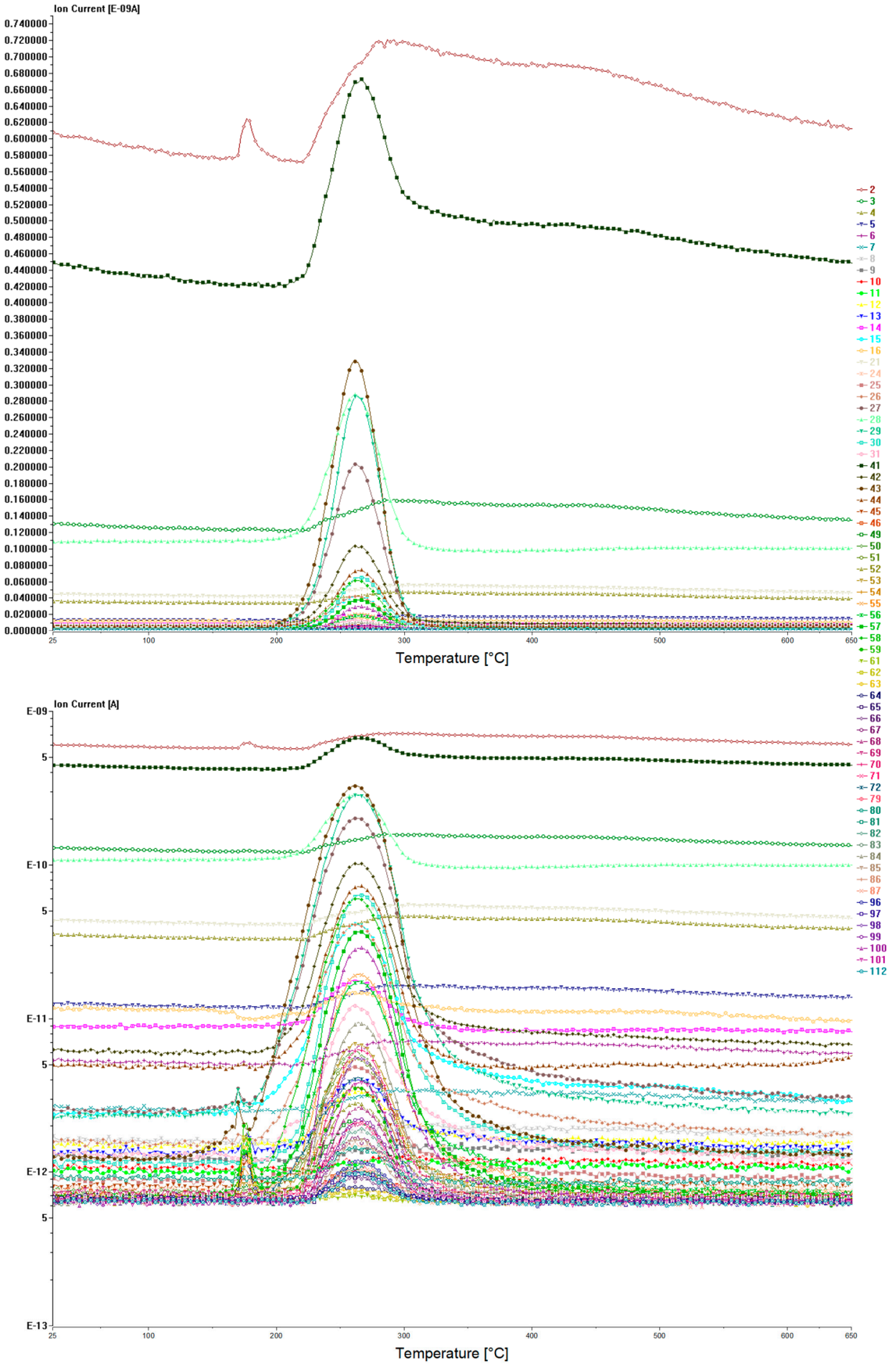

Figure S13. MS spectrum for **Yb** sample. Top: linear scale; bottom: logarithmic scale; right: m/z value legend.

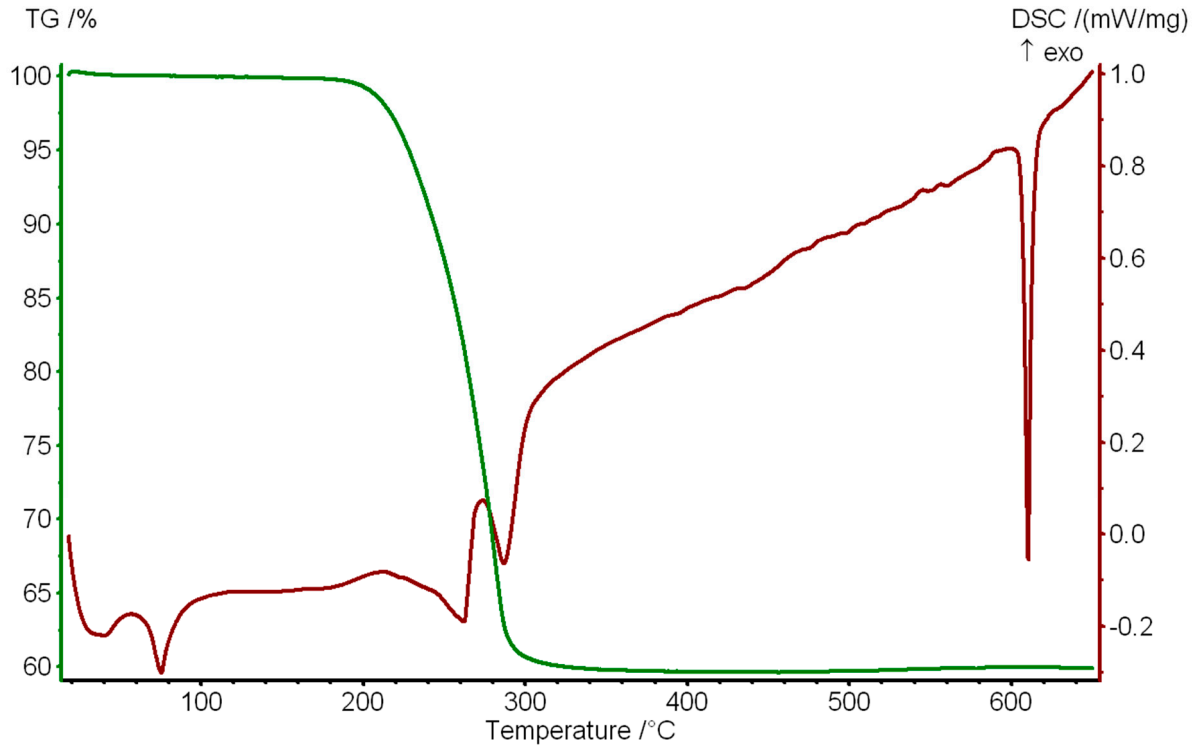

Figure S14. TGA/DSC curves for **Ho** sample.

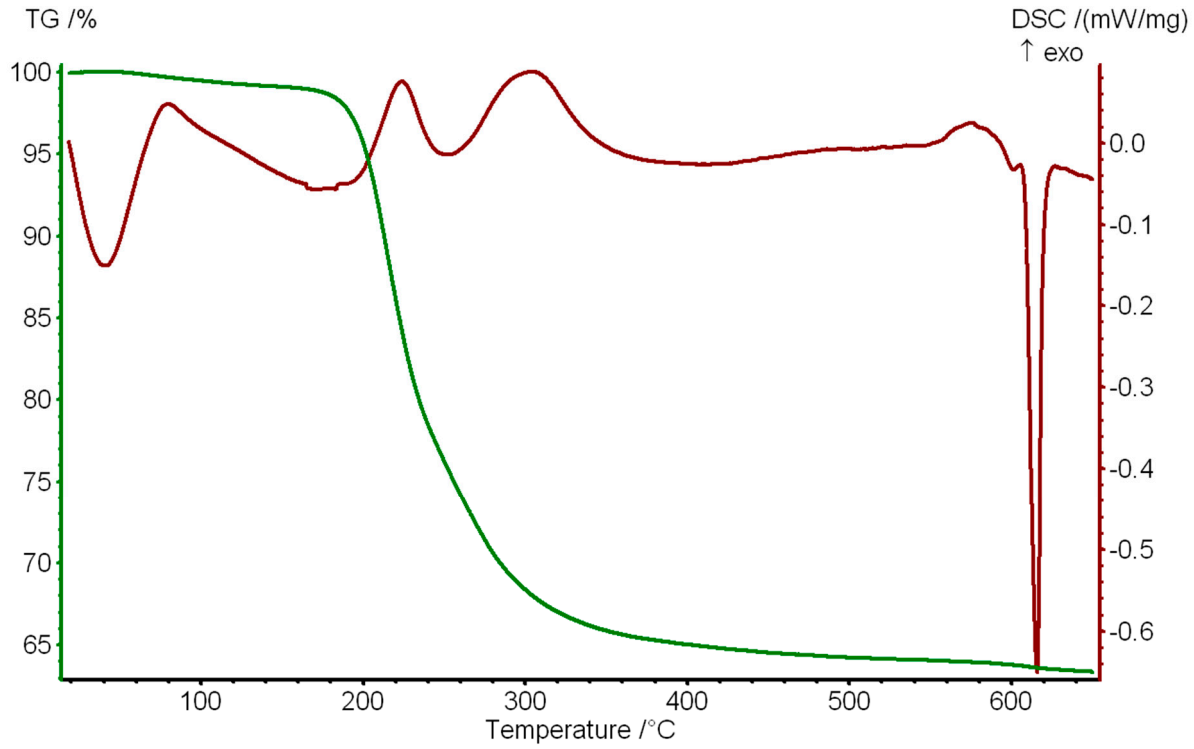

Figure S15. TGA/DSC curves for **Tm** sample.

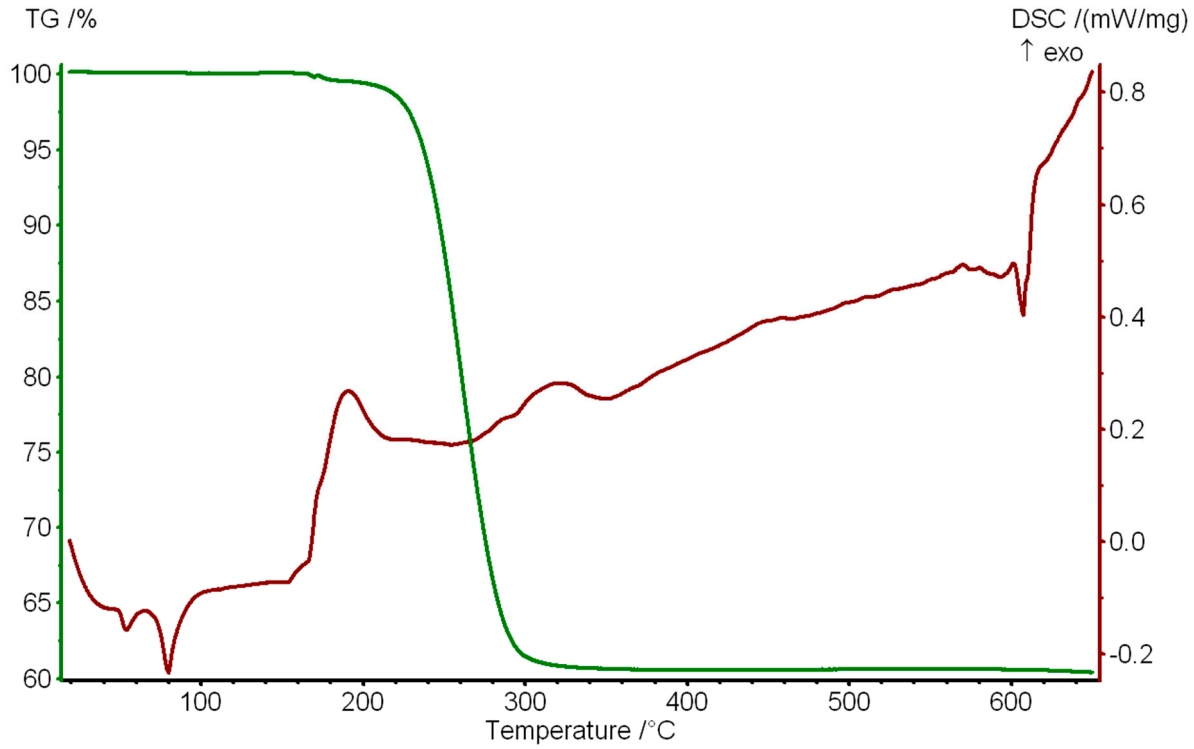

Figure S16. TGA/DSC curves for **Yb** sample.

3. Solid decomposition products

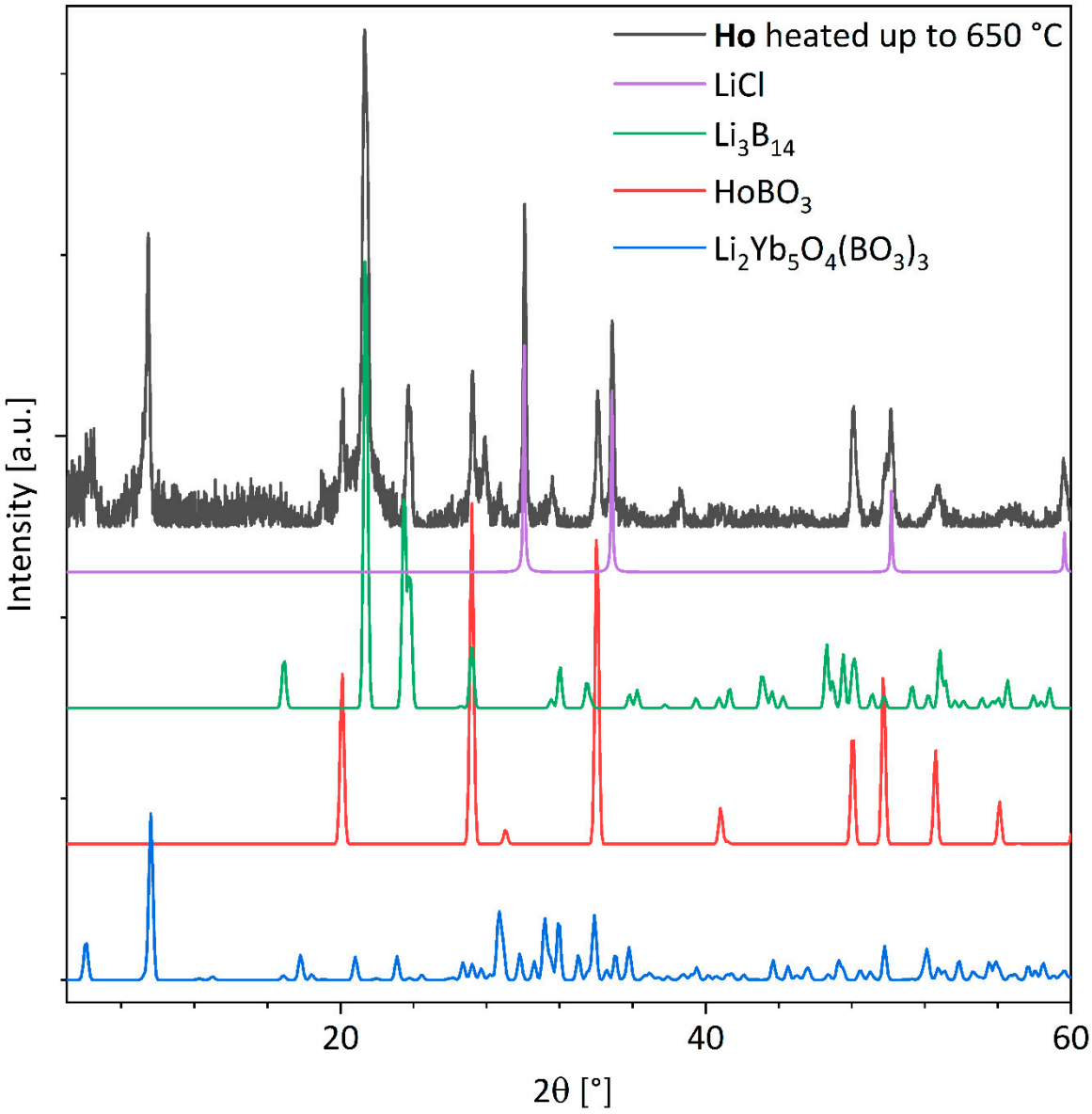

Figure S17. PXRD pattern (with subtracted background) of **Ho** sample heated to 650 °C, and simulated patterns of identified crystalline pyrolysis products [66-69].

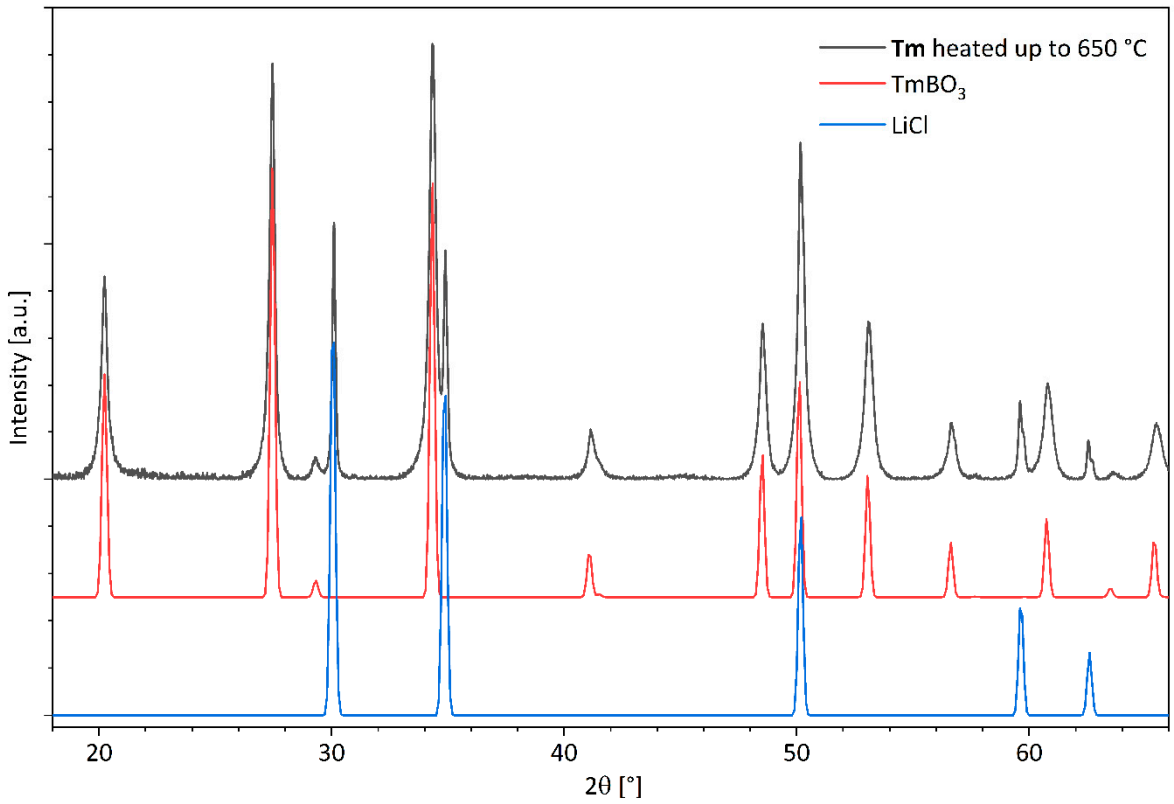

Figure S18. PXRD pattern (with subtracted background) of **Tm** sample heated to 650 °C, and simulated patterns of identified crystalline pyrolysis products [67,69].

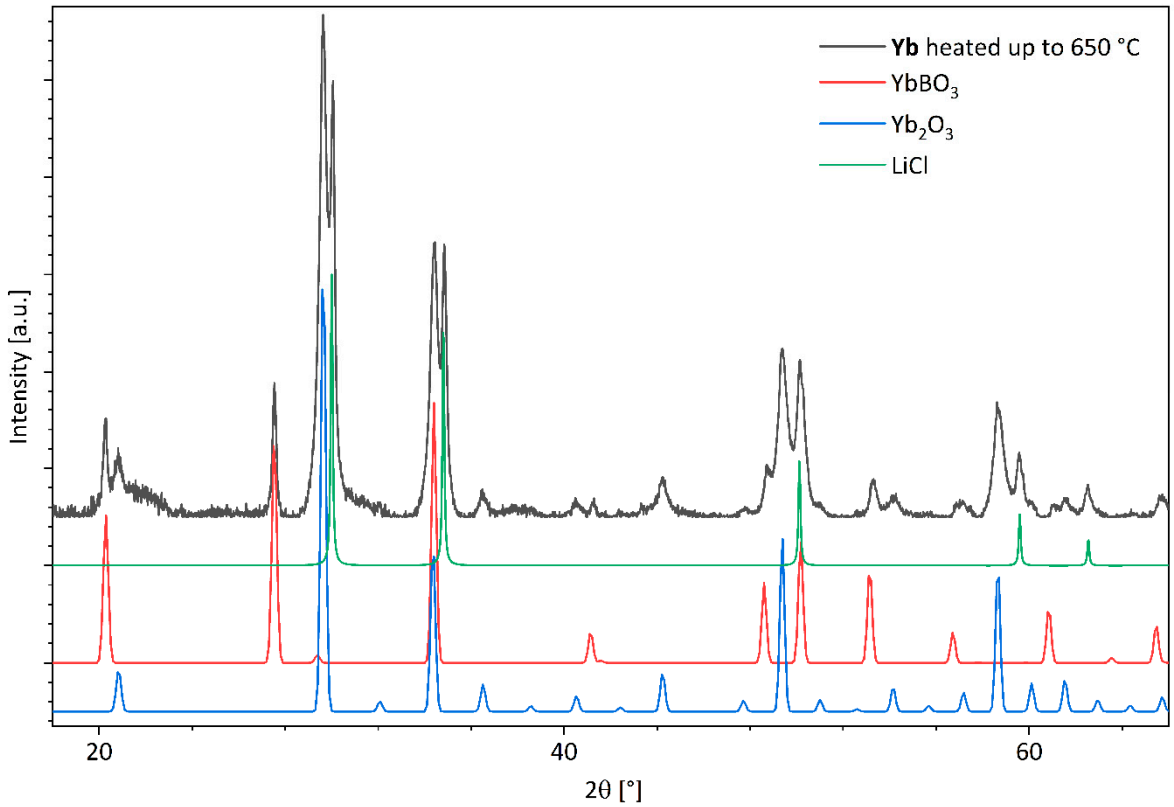

Figure S19. PXRD pattern (with subtracted background) of **Yb** sample heated to 650 °C, and simulated patterns of identified crystalline pyrolysis products [67,69,70].

4. Preliminary CIF of α-TBAHoB from SC-XRD data (100 K)

```
data_Ho_3
_audit_creation_date                    2020-12-14
_audit_creation_method
;
Olex2 1.2
(compiled 2018.05.29 svn.r3508 for OlexSys, GUI svn.r5506)
;
_audit_contact_author_address           ?
_audit_contact_author_email             ?
_audit_contact_author_name               ''
_audit_contact_author_phone              ?
_publ_contact_author_id_orcid           ?
_publ_section_references
;
Bourhis, L.J., Dolomanov, O.V., Gildea, R.J., Howard, J.A.K., Puschmann, H.
 (2015). Acta Cryst. A71, 59-75.

Dolomanov, O.V., Bourhis, L.J., Gildea, R.J, Howard, J.A.K. & Puschmann, H.
 (2009), J. Appl. Cryst. 42, 339-341.

Sheldrick, G.M. (2015). Acta Cryst. A71, 3-8.
;
_chemical_formula_moiety                'B4 H16 Ho, C16 H36 N'
_chemical_formula_sum                    'C16 H52 B4 Ho N'
_chemical_formula_weight                466.83
_chemical_oxdiff_formula                'Ho B4 N C16 H52'
_chemical_oxdiff_usercomment             '100 K '
loop_
   _atom_type_symbol
   _atom_type_scat_dispersion_real
   _atom_type_scat_dispersion_imag
   _atom_type_scat_Cromer_Mann_a1
   _atom_type_scat_Cromer_Mann_a2
   _atom_type_scat_Cromer_Mann_a3
   _atom_type_scat_Cromer_Mann_a4
   _atom_type_scat_Cromer_Mann_b1
   _atom_type_scat_Cromer_Mann_b2
   _atom_type_scat_Cromer_Mann_b3
   _atom_type_scat_Cromer_Mann_b4
   _atom_type_scat_Cromer_Mann_c
```

```
   _atom_type_scat_source
   _atom_type_scat_dispersion_source
  H 0.00000 0.00000 0.49300 0.32291 0.14019 0.04081 10.51090 26.12570 3.14236
  57.79970 0.0030380000826
  'International Tables Volume C Table 6.1.1.4 (pp. 500-502)'
  'Henke, Gullikson and Davis, At. Data and Nucl. Data Tables, 1993, 54, 2'
  C 0.01920 0.00962 2.31000 1.02000 1.58860 0.86500 20.84390 10.20750 0.56870
  51.65120 0.215599998832
  'International Tables Volume C Table 6.1.1.4 (pp. 500-502)'
  'Henke, Gullikson and Davis, At. Data and Nucl. Data Tables, 1993, 54, 2'
  B 0.00963 0.00408 2.05450 1.33260 1.09790 0.70680 23.21850 1.02100 60.34980
  0.14030 -0.193200007081
  'International Tables Volume C Table 6.1.1.4 (pp. 500-502)'
  'Henke, Gullikson and Davis, At. Data and Nucl. Data Tables, 1993, 54, 2'
  Ho -15.55474 4.01359 26.90490 17.29400 14.55830 3.63837 2.07051 0.19794 11.44070
  92.65660 4.56795978546
  'International Tables Volume C Table 6.1.1.4 (pp. 500-502)'
  'Henke, Gullikson and Davis, At. Data and Nucl. Data Tables, 1993, 54, 2'
  N 0.03256 0.01839 12.21260 3.13220 2.01250 1.16630 0.00570 9.89330 28.99750
  0.58260 -11.5290002823
  'International Tables Volume C Table 6.1.1.4 (pp. 500-502)'
  'Henke, Gullikson and Davis, At. Data and Nucl. Data Tables, 1993, 54, 2'

_space_group_crystal_system          'monoclinic'
_space_group_IT_number                 14
_space_group_name_H-M_alt              'P 1 21/n 1'
_space_group_name_Hall                 '-P 2ybc (x-z,y,z)'
loop_
   _space_group_symop_id
   _space_group_symop_operation_xyz
  1 x,y,z
  2 -x+1/2,y+1/2,-z+1/2
  3 -x,-y,-z
  4 x-1/2,-y-1/2,z-1/2

_symmetry_Int_Tables_number          14
_cell_length_a                       11.0380(13)
_cell_length_b                       20.019(2)
_cell_length_c                       11.7510(13)
_cell_angle_alpha                    90
_cell_angle_beta                     99.643(12)
_cell_angle_gamma                      90
```

```
_cell_volume                          2559.9(5)
_cell_formula_units_Z                 4
_cell_measurement_reflns_used         2465
_cell_measurement_temperature         100.01(10)
_cell_measurement_theta_max           53.3510
_cell_measurement_theta_min           4.1310
_exptl_absorpt_coefficient_mu         5.705
_exptl_absorpt_correction_T_max       0.11351
_exptl_absorpt_correction_T_min       0.04401
_exptl_absorpt_correction_type        sphere
_exptl_absorpt_process_details
;
CrysAlisPro 1.171.39.46 (Rigaku Oxford Diffraction, 2018)
Spherical absorption correction
  using equivalent radius and absorption coefficient.
Empirical absorption correction using spherical harmonics,
  implemented in SCALE3 ABSPACK scaling algorithm.
;
_exptl_crystal_colour                 'clear colourless'
_exptl_crystal_colour_lustre          clear
_exptl_crystal_colour_modifier        .
_exptl_crystal_colour_primary         colourless
_exptl_crystal_density_diffrn         1.2111
_exptl_crystal_description            block
_exptl_crystal_F_000                  907.1993
_diffrn_reflns_av_R_equivalents       0.1682
_diffrn_reflns_av_unetI/netI          0.1386
_diffrn_reflns_limit_h_max            11
_diffrn_reflns_limit_h_min            -11
_diffrn_reflns_limit_k_max            15
_diffrn_reflns_limit_k_min            -21
_diffrn_reflns_limit_l_max            12
_diffrn_reflns_limit_l_min            -10
_diffrn_reflns_number                 10865
_diffrn_reflns_theta_full             55.7871
_diffrn_reflns_theta_max              55.79
_diffrn_reflns_theta_min              4.41
_diffrn_ambient_environment           N~2~
_diffrn_ambient_temperature           100.01(10)
_diffrn_detector                      'CCD plate'
_diffrn_detector_area_resol_mean      5.2687
_diffrn_detector_type                 Atlas
```

```
_diffrn_measured_fraction_theta_full    0.9746
_diffrn_measured_fraction_theta_max    0.9746
_diffrn_measurement_details
;
List of Runs (angles in degrees, time in seconds):

   # Type      Start       End    Width   t~exp~     \w        \q        \k        \f     Frames
------------------------------------------------------------------------------
   1   \w     -84.00 -39.00     1.00      4.00      --      0.00 178.00 150.00      45
   2   \w     -22.00   71.00     1.00      4.00      --      0.00   38.00   90.00      93
   3   \w     -22.00   71.00     1.00      4.00      --      0.00   38.00-180.00      93
   4   \w      32.00 106.00     1.00     16.00      --     68.24 -99.00   30.00      74
   5   \w      -2.00   94.00     1.00     16.00      --     68.24 -57.00   90.00      96
   6   \w      54.00 112.00     1.00     16.00      --     68.24-125.00-180.00      58
   7   \w      -2.00   94.00     1.00     16.00      --     68.24 -57.00-180.00      96
   8   \w      -3.00   90.00     1.00     16.00      --     68.24 -38.00-120.00      93
   9   \w      -8.00 104.00     1.00     16.00      --     68.24 -19.00 120.00     112
  10   \w      -3.00   90.00     1.00     16.00      --     68.24 -38.00     0.00      93
  11   \w      32.00   77.00     1.00     16.00      --     68.24 -99.00 -30.00      45
;
_diffrn_measurement_device              'four-circle diffractometer'
_diffrn_measurement_device_type
  'SuperNova, Single source at offset/far, Atlas'
_diffrn_measurement_method              '\w scans'
_diffrn_orient_matrix_type
  'CrysAlisPro convention (1999,Acta A55,543-557)'
_diffrn_orient_matrix_UB_11             -0.1279046000
_diffrn_orient_matrix_UB_12             -0.0124396000
_diffrn_orient_matrix_UB_13             0.0318861000
_diffrn_orient_matrix_UB_21             -0.0260076000
_diffrn_orient_matrix_UB_22             -0.0531177000
_diffrn_orient_matrix_UB_23             -0.0958200000
_diffrn_orient_matrix_UB_31             0.0546008000
_diffrn_orient_matrix_UB_32             -0.0543211000
_diffrn_orient_matrix_UB_33             0.0865516000
_diffrn_radiation_monochromator         mirror
_diffrn_radiation_probe                 x-ray
_diffrn_radiation_type                  'Cu K\a'
_diffrn_radiation_wavelength            1.54184
_diffrn_source                          'micro-focus sealed X-ray tube'
_diffrn_source_type                     'SuperNova (Cu) X-ray Source'
_reflns_Friedel_coverage                0.0
```

```
_reflns_limit_h_max                 7
_reflns_limit_h_min                 -11
_reflns_limit_k_max                 21
_reflns_limit_k_min                 0
_reflns_limit_l_max                 12
_reflns_limit_l_min                 -7
_reflns_number_gt                   1741
_reflns_number_total                3228
_reflns_odcompleteness_completeness 98.43
_reflns_odcompleteness_iscentric    1
_reflns_odcompleteness_theta        54.18
_reflns_threshold_expression        I>=2u(I)
_computing_cell_refinement          'CrysAlisPro 1.171.39.46 (Rigaku OD, 2018)'
_computing_data_collection          'CrysAlisPro 1.171.39.46 (Rigaku OD, 2018)'
_computing_data_reduction           'CrysAlisPro 1.171.39.46 (Rigaku OD, 2018)'
_computing_molecular_graphics       'Olex2 (Dolomanov et al., 2009)'
_computing_publication_material     'Olex2 (Dolomanov et al., 2009)'
_computing_structure_refinement     'olex2.refine (Bourhis et al., 2015)'
_computing_structure_solution       'ShelXT (Sheldrick, 2015)'
_refine_diff_density_max            5.7607
_refine_diff_density_min            -3.1144
_refine_diff_density_rms            0.4787
_refine_ls_d_res_high               0.9322
_refine_ls_d_res_low                10.0270
_refine_ls_goodness_of_fit_ref      1.6461
_refine_ls_hydrogen_treatment       mixed
_refine_ls_matrix_type              full
_refine_ls_number_constraints       53
_refine_ls_number_parameters        252
_refine_ls_number_reflns            3228
_refine_ls_number_restraints        40
_refine_ls_R_factor_all             0.2576
_refine_ls_R_factor_gt              0.1996
_refine_ls_restrained_S_all         1.6352
_refine_ls_shift/su_max             0.0767
_refine_ls_shift/su_mean            0.0038
_refine_ls_structure_factor_coef    Fsqd
_refine_ls_weighting_details
 'w=1/[\s^2^(Fo^2^)+(0.2P)^2^] where P=(Fo^2^+2Fc^2^)/3'
_refine_ls_weighting_scheme         calc
_refine_ls_wR_factor_gt             0.4724
_refine_ls_wR_factor_ref            0.5140
```

_olex2_refinement_description
;
1. Fixed Uiso
 At 1.2 times of:
  All C(H,H) groups
 At 1.5 times of:
  All C(H,H,H) groups
2. Restrained distances
 B00L-H5aa \\sim B00L-Hl \\sim B00L-Hq \\sim B00L-Hp \\sim B00M-H6aa \\sim
B00M-Hf \\sim B00M-Hi ~
 B00I-Hh \\sim B00I-H3aa \\sim B00I-Hj \\sim B00I-Hm \\sim B00M-Hn \\sim
B00J-Ho \\sim B00J-H4aa \\sim B00J-
 Hg \\sim B00J-Hk
 with sigma of 0.01
3. Restrained angles
 Hk-B00J-Ho
 fixed at 109.471 with sigma of 0.02
 Hk-B00J-H4aa
 fixed at 109.471 with sigma of 0.02
 Hk-B00J-Hg
 fixed at 109.471 with sigma of 0.02
 Ho-B00J-H4aa
 fixed at 109.471 with sigma of 0.02
 Ho-B00J-Hg
 fixed at 109.471 with sigma of 0.02
 H4aa-B00J-Hg
 fixed at 109.471 with sigma of 0.02
 H3aa-B00I-Hj
 fixed at 109.471 with sigma of 0.02
 H3aa-B00I-Hm
 fixed at 109.471 with sigma of 0.02
 H3aa-B00I-Hh
 fixed at 109.471 with sigma of 0.02
 Hj-B00I-Hm
 fixed at 109.471 with sigma of 0.02
 Hj-B00I-Hh
 fixed at 109.471 with sigma of 0.02
 Hm-B00I-Hh
 fixed at 109.471 with sigma of 0.02
 Hp-B00L-Hq
 fixed at 109.471 with sigma of 0.02
 Hp-B00L-Hl

fixed at 109.471 with sigma of 0.02
Hp-B00L-H5aa
fixed at 109.471 with sigma of 0.02
Hq-B00L-Hl
fixed at 109.471 with sigma of 0.02
Hq-B00L-H5aa
fixed at 109.471 with sigma of 0.02
Hl-B00L-H5aa
fixed at 109.471 with sigma of 0.02
Hf-B00M-H6aa
fixed at 109.471 with sigma of 0.02
Hf-B00M-Hi
fixed at 109.471 with sigma of 0.02
Hf-B00M-Hn
fixed at 109.471 with sigma of 0.02
H6aa-B00M-Hi
fixed at 109.471 with sigma of 0.02
H6aa-B00M-Hn
fixed at 109.471 with sigma of 0.02
Hi-B00M-Hn
fixed at 109.471 with sigma of 0.02
4. Uiso/Uaniso restraints and constraints
Uiso(Hk) = Uiso(H4aa) = Uiso(Ho) = Uiso(Hg) = Uiso(Hp) = Uiso(Hq) = Uiso(Hl) =
Uiso(H5aa) = Uiso(H6aa) = Uiso(Hf) = Uiso(Hn) = Uiso(Hi) = Uiso(Hh) =
Uiso(H3aa) = Uiso(Hj) = Uiso(Hm)
5.a Secondary CH2 refined with riding coordinates:
C003(H00a,H00b), C004(H00c,H00d), C005(H00e,H00f), C006(H00g,H00h), C007(H00i,
H00j), C008(H00k,H00l), C00A(H00p,H00q), C00B(H00r,H00s), C00E(H00z,H),
C00F(H00,Ha), C00G(H0aa,Hb), C00H(H1aa,Hc)
5.b Idealised Me refined as rotating group:
C009(H00m,H00n,H00o), C00C(H00t,H00u,H00v), C00D(H00w,H00x,H00y), C00K(H2aa,
Hd,He)
;
_atom_sites_solution_primary dual
loop_
_atom_site_label
_atom_site_type_symbol
_atom_site_fract_x
_atom_site_fract_y
_atom_site_fract_z
_atom_site_U_iso_or_equiv
_atom_site_adp_type

```
  _atom_site_occupancy
  _atom_site_refinement_flags_posn
Ho01 Ho 0.79220(19) 0.68774(10) 0.46389(19) 0.0662(11) Uani 1.000000 .
N002 N 0.2623(18) 0.6236(11) 0.3505(17) 0.053(6) Uani 1.000000 .
C003 C 0.279(2) 0.7493(14) 0.374(3) 0.059(7) Uani 1.000000 .
H00a H 0.327(2) 0.7455(14) 0.450(3) 0.071(9) Uiso 1.000000 R
H00b H 0.335(2) 0.7504(14) 0.319(3) 0.071(9) Uiso 1.000000 R
C004 C 0.326(3) 0.6174(16) 0.248(2) 0.068(8) Uani 1.000000 .
H00c H 0.267(3) 0.6279(16) 0.180(2) 0.082(10) Uiso 1.000000 R
H00d H 0.389(3) 0.6513(16) 0.255(2) 0.082(10) Uiso 1.000000 R
C005 C 0.384(3) 0.5513(16) 0.227(3) 0.078(10) Uani 1.000000 .
H00e H 0.446(3) 0.5406(16) 0.293(3) 0.094(12) Uiso 1.000000 R
H00f H 0.322(3) 0.5166(16) 0.220(3) 0.094(12) Uiso 1.000000 R
C006 C 0.446(3) 0.5525(16) 0.115(2) 0.074(9) Uani 1.000000 .
H00g H 0.470(3) 0.5073(16) 0.100(2) 0.088(11) Uiso 1.000000 R
H00h H 0.383(3) 0.5653(16) 0.051(2) 0.088(11) Uiso 1.000000 R
C007 C 0.079(2) 0.5583(16) 0.232(2) 0.065(8) Uani 1.000000 .
H00i H 0.032(2) 0.5992(16) 0.214(2) 0.078(9) Uiso 1.000000 R
H00j H 0.124(2) 0.5492(16) 0.170(2) 0.078(9) Uiso 1.000000 R
C008 C 0.198(2) 0.6894(12) 0.3501(19) 0.045(6) Uani 1.000000 .
H00k H 0.147(2) 0.6951(12) 0.2754(19) 0.054(7) Uiso 1.000000 R
H00l H 0.144(2) 0.6878(12) 0.4074(19) 0.054(7) Uiso 1.000000 R
C009 C -0.091(3) 0.4830(15) 0.138(3) 0.080(10) Uani 1.000000 .
H00m H -0.045(4) 0.463(10) 0.085(8) 0.120(14) Uiso 1.000000 GR
H00n H -0.152(13) 0.452(9) 0.156(4) 0.120(14) Uiso 1.000000 GR
H00o H -0.131(16) 0.523(2) 0.104(11) 0.120(14) Uiso 1.000000 GR
C00A C 0.207(3) 0.8140(13) 0.365(3) 0.063(8) Uani 1.000000 .
H00p H 0.161(3) 0.8181(13) 0.287(3) 0.075(9) Uiso 1.000000 R
H00q H 0.147(3) 0.8113(13) 0.417(3) 0.075(9) Uiso 1.000000 R
C00B C 0.169(2) 0.5660(15) 0.349(2) 0.064(8) Uani 1.000000 .
H00r H 0.213(2) 0.5244(15) 0.365(2) 0.077(9) Uiso 1.000000 R
H00s H 0.121(2) 0.5733(15) 0.410(2) 0.077(9) Uiso 1.000000 R
C00C C 0.283(3) 0.8772(16) 0.394(3) 0.093(11) Uani 1.000000 .
H00t H 0.335(17) 0.884(7) 0.337(12) 0.139(17) Uiso 1.000000 GR
H00u H 0.229(3) 0.915(3) 0.39(2) 0.139(17) Uiso 1.000000 GR
H00v H 0.333(18) 0.873(5) 0.469(10) 0.139(17) Uiso 1.000000 GR
C00D C 0.552(2) 0.5963(14) 0.114(2) 0.064(8) Uani 1.000000 .
H00w H 0.558(10) 0.608(8) 0.036(3) 0.096(12) Uiso 1.000000 GR
H00x H 0.543(8) 0.636(4) 0.157(13) 0.096(12) Uiso 1.000000 GR
H00y H 0.626(3) 0.573(3) 0.149(14) 0.096(12) Uiso 1.000000 GR
C00E C 0.310(2) 0.6162(13) 0.572(2) 0.052(7) Uani 1.000000 .
H00z H 0.259(2) 0.5773(13) 0.578(2) 0.063(8) Uiso 1.000000 R
```

H H 0.261(2) 0.6559(13) 0.577(2) 0.063(8) Uiso 1.000000 R
C00F C -0.007(3) 0.5009(15) 0.246(3) 0.078(9) Uani 1.000000 .
H00 H 0.042(3) 0.4620(15) 0.273(3) 0.093(11) Uiso 1.000000 R
Ha H -0.056(3) 0.5125(15) 0.305(3) 0.093(11) Uiso 1.000000 R
C00G C 0.420(3) 0.6158(17) 0.669(2) 0.077(9) Uani 1.000000 .
H0aa H 0.476(3) 0.5805(17) 0.655(2) 0.092(11) Uiso 1.000000 R
Hb H 0.463(3) 0.6581(17) 0.670(2) 0.092(11) Uiso 1.000000 R
C00H C 0.358(2) 0.6153(15) 0.463(2) 0.062(8) Uani 1.000000 .
H1aa H 0.401(2) 0.5733(15) 0.459(2) 0.074(9) Uiso 1.000000 R
Hc H 0.418(2) 0.6508(15) 0.466(2) 0.074(9) Uiso 1.000000 R
B00I B 0.654(3) 0.7768(17) 0.508(3) 0.066(9) Uani 1.000000 D
B00J B 0.685(2) 0.5817(15) 0.467(3) 0.053(8) Uani 1.000000 D
C00K C 0.378(3) 0.6048(17) 0.783(2) 0.075(9) Uani 1.000000 .
H2aa H 0.349(18) 0.560(3) 0.787(8) 0.113(14) Uiso 1.000000 GR
Hd H 0.446(5) 0.612(10) 0.844(2) 0.113(14) Uiso 1.000000 GR
He H 0.313(13) 0.635(7) 0.790(8) 0.113(14) Uiso 1.000000 GR
B00L B 0.982(2) 0.6864(18) 0.615(3) 0.075(11) Uani 1.000000 D
B00M B 0.849(3) 0.701(2) 0.273(4) 0.094(14) Uani 1.000000 D
H4aa H 0.796(7) 0.614(7) 0.473(13) 0.069(19) Uiso 1.000000 D
H6aa H 0.952(8) 0.738(6) 0.315(12) 0.069(19) Uiso 1.000000 D
Hf H 0.828(13) 0.656(6) 0.356(9) 0.069(19) Uiso 1.000000 D
H3aa H 0.704(13) 0.732(5) 0.592(9) 0.069(19) Uiso 1.000000 D
Hg H 0.654(13) 0.579(7) 0.575(6) 0.069(19) Uiso 1.000000 D
Hh H 0.726(11) 0.780(8) 0.424(9) 0.069(19) Uiso 1.000000 D
Hi H 0.866(13) 0.668(7) 0.175(8) 0.069(19) Uiso 1.000000 D
Hj H 0.537(6) 0.756(7) 0.461(12) 0.069(19) Uiso 1.000000 D
Hk H 0.695(14) 0.518(3) 0.426(12) 0.069(19) Uiso 1.000000 D
H5aa H 0.966(13) 0.744(4) 0.552(10) 0.069(19) Uiso 1.000000 D
Hl H 1.010(13) 0.635(5) 0.547(9) 0.069(19) Uiso 1.000000 D
Hm H 0.649(14) 0.839(3) 0.557(11) 0.069(19) Uiso 1.000000 D
Hn H 0.749(8) 0.743(6) 0.248(13) 0.069(19) Uiso 1.000000 D
Ho H 0.596(10) 0.616(6) 0.394(10) 0.069(19) Uiso 1.000000 D
Hp H 0.875(8) 0.672(7) 0.656(12) 0.069(19) Uiso 1.000000 D
Hq H 1.076(9) 0.695(7) 0.707(9) 0.069(19) Uiso 1.000000 D

loop_
_atom_site_aniso_label
_atom_site_aniso_U_11
_atom_site_aniso_U_22
_atom_site_aniso_U_33
_atom_site_aniso_U_12
_atom_site_aniso_U_13

_atom_site_aniso_U_23
Ho01 0.0520(13) 0.0827(19) 0.0601(16) -0.0003(11) -0.0017(10) -0.0014(11)
N002 0.044(12) 0.073(16) 0.040(13) -0.004(10) 0.001(10) 0.003(10)
C003 0.045(15) 0.08(2) 0.056(18) -0.002(14) 0.028(13) -0.006(14)
C004 0.062(18) 0.10(3) 0.035(15) -0.012(16) -0.006(13) 0.006(14)
C005 0.065(19) 0.09(2) 0.06(2) 0.014(17) -0.026(16) -0.001(16)
C006 0.08(2) 0.10(2) 0.030(15) 0.003(17) -0.029(14) 0.012(14)
C007 0.058(17) 0.10(2) 0.031(14) -0.004(16) -0.001(12) 0.011(14)
C008 0.033(12) 0.070(17) 0.026(13) 0.008(12) -0.009(9) -0.012(11)
C009 0.058(18) 0.09(2) 0.09(2) -0.002(15) -0.006(17) 0.016(17)
C00A 0.069(19) 0.057(18) 0.065(19) -0.000(15) 0.019(15) -0.007(14)
C00B 0.053(16) 0.09(2) 0.049(17) -0.008(15) -0.003(13) -0.002(14)
C00C 0.10(3) 0.09(2) 0.10(3) 0.04(2) 0.01(2) 0.01(2)
C00D 0.039(14) 0.10(2) 0.056(18) 0.001(14) 0.012(13) -0.006(15)
C00E 0.031(12) 0.059(17) 0.063(17) 0.002(11) -0.004(12) 0.000(13)
C00F 0.050(17) 0.08(2) 0.09(2) 0.004(15) -0.003(16) -0.002(18)
C00G 0.063(18) 0.12(3) 0.042(17) 0.003(18) 0.009(14) -0.008(16)
C00H 0.042(15) 0.10(2) 0.045(16) 0.009(14) 0.008(12) 0.001(14)
B00I 0.08(2) 0.08(3) 0.034(18) 0.012(19) 0.007(16) -0.005(15)
B00J 0.036(15) 0.08(2) 0.050(19) 0.003(14) 0.012(13) 0.001(15)
C00K 0.061(18) 0.12(3) 0.037(16) -0.004(17) -0.000(13) 0.008(15)
B00L 0.025(14) 0.13(3) 0.05(2) 0.011(16) -0.040(14) 0.001(19)
B00M 0.036(18) 0.12(4) 0.14(4) 0.002(18) 0.04(2) 0.02(3)

5. FTIR spectra of as-milled samples.

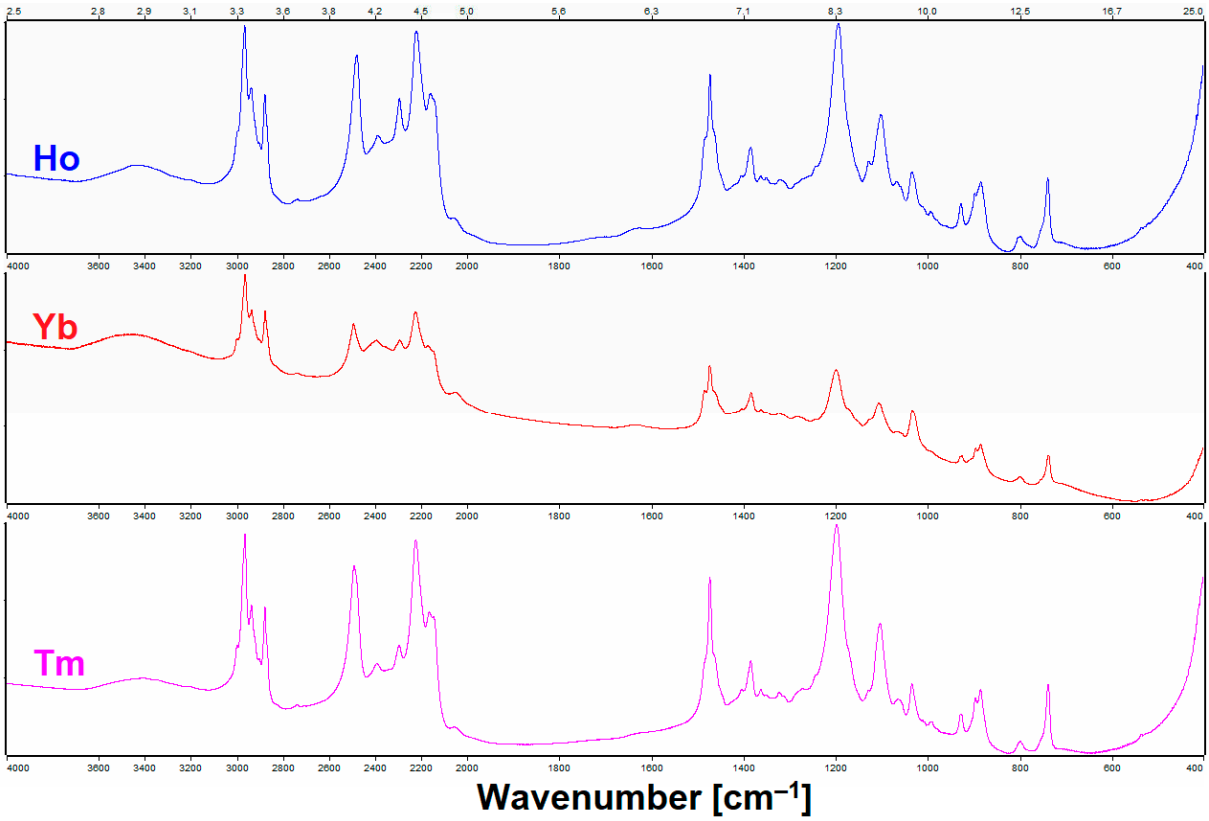

Figure S20. FTIR spectra of **Ho, Yb** and **Tm** as-milled samples.